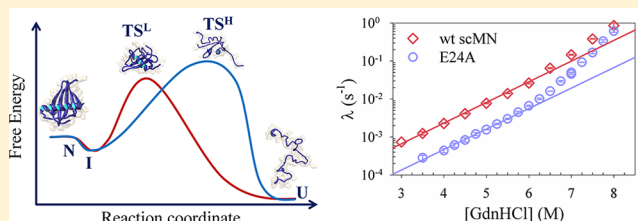


# The Utilization of Competing Unfolding Pathways of Monellin Is Dictated by Enthalpic Barriers

Nilesh Aghera and Jayant B. Udgaonkar\*

National Centre for Biological Sciences, Tata Institute of Fundamental Research, Bangalore 560065, India

**ABSTRACT:** Direct evidence of the presence of competing pathways for the folding or unfolding reactions of proteins is difficult to obtain. A direct signature for multiple pathways, seen so far only rarely in folding or unfolding studies, is an upward curvature in the dependence of the logarithm of the observed rate constant ( $\lambda_U$ ) of folding on denaturant concentration. In this study, the unfolding mechanism of the wild-type (wt) and E24A variants of monellin has been investigated, and both variants are shown to display upward curvatures in plots of  $\log \lambda_U$  versus denaturant concentration. Curvature is distinctly more pronounced for E24A than for the wt protein. Kinetic unfolding studies of E24A were conducted over a range of denaturant concentrations and across a range of temperatures, and the kinetic data were globally analyzed assuming two parallel pathways L and H, which proceed through transition states  $TS^L$  and  $TS^H$ , respectively. The observation of the upward curvature in the unfolding kinetics permitted a thermodynamic analysis of how unfolding switches from one pathway to the other upon a change in unfolding conditions. The  $m_{\ddagger-N}$  and  $\Delta C_p^\ddagger$  values indicate that  $TS^L$  is more compact than  $TS^H$ . The major contribution to the free energy of activation on either pathway is seen to be enthalpic and not entropic in origin.



The availability of multiple pathways by which a protein can fold adds robustness to the folding process.<sup>1,2</sup> The possibility that a large multitude of pathways might indeed be available to a protein for folding has been elegantly revealed by the application of statistical mechanics theory to protein folding.<sup>3</sup> Nevertheless, relatively few experimental studies have been able to demonstrate that multiple pathways can be concurrently used by a protein for folding or unfolding.<sup>2,4–19</sup> The detection of heterogeneity in the structures of the states populated at different stages of folding or unfolding by the use of high-resolution probes<sup>2,16,20–25</sup> and the realization that this heterogeneity can be modulated either by a change in folding conditions or by mutation of the protein sequence have made it possible to demonstrate that the folding pathway can be structurally distinct under a different folding condition,<sup>26–35</sup> or for a mutant variant of the same protein.<sup>36–38</sup> Determining how competing pathways differ in the sequence of structural events defining them remains a difficult task. In particular, it is important to determine how the rate-limiting steps differ or how the energetics and structures of the transition states (TSs) on different pathways differ, to determine when and how folding or unfolding reactions might switch from one pathway to another. So far, such studies have been conducted with only the I27 domain of titin.<sup>39</sup>

Detailed thermodynamic analysis<sup>39–44</sup> in terms of activation parameters  $\Delta H^\ddagger$ ,  $\Delta S^\ddagger$ , and  $\Delta C_p^\ddagger$  provides a general picture of the extent of burial of hydrophobic residues and packing interactions in the TS. Such characterization requires a study of the temperature dependence of the folding or unfolding kinetics.<sup>39,40,43–45</sup> The thermodynamic characterization of TSs on parallel pathways is important for understanding what drives

the formation of, and stabilizes, different structural forms from the same sequence and under the same conditions. Switching between competing pathways upon modulation of folding or unfolding conditions will depend on how the thermodynamic activation parameters governing the pathways differ, and the detection of such switching may be facilitated by changing the environmental conditions.

When only a single pathway is operative, the logarithm of the rate constant of folding or unfolding of a protein has a linear dependence on denaturant concentration; however, when an intermediate is populated, a downward curvature may be observed.<sup>46–48</sup> A direct signature for competing pathways is an upward curvature in the denaturant dependence of the logarithm of the observed rate constant of folding or unfolding.<sup>5,9</sup> Nevertheless, even when a protein uses competing pathways to fold or unfold, it may or may not show such upward curvature, which manifests itself only when their TSs differ subtly in their energies and structures. If the pathways do not differ in the dependences of their free energies of activation,  $\Delta G^\ddagger$ , on denaturant concentration, an upward curvature will not be seen. When a protein does fold using multiple pathways but the upward curvature is not seen in the kinetics of the wild-type protein, it is possible that certain mutations, which differentially affect the free energies and structures of the TSs, may cause an upward curvature to manifest itself.<sup>5</sup>

The small plant protein, monellin, has been extensively used in its natural double-chain (dcMN) form and its artificially

Received: May 30, 2013

Revised: July 30, 2013

Published: July 31, 2013

created single-chain (scMN) form to study the thermodynamics and kinetics of folding and unfolding processes. Both variants of monellin are reported to utilize multiple pathways in their folding or unfolding processes.<sup>7–9</sup> Parallel pathways for the refolding of dcMN were revealed by the presence of upward curvature in the dependence of the logarithm of the observed folding rate constant on denaturant concentration.<sup>9</sup> In the case of scMN, the direct signature of an upward curvature was not seen in the dependence of the logarithm of the rate constant on denaturant concentration, for folding or for unfolding.<sup>7,8,49</sup> Parallel pathways for the folding and unfolding of scMN could, however, be detected by using interrupted folding and unfolding studies<sup>8</sup> and could be confirmed both by the use of time-resolved Förster resonance energy transfer (FRET) measurements<sup>49</sup> and by the use of thiol labeling measurements coupled to mass spectrometry.<sup>7</sup> Approximately 25% of the protein molecules were found to utilize the slow pathway in the absence of denaturant.<sup>7</sup> It was, however, not possible, in the absence of the direct signature, to understand the physical origin of the parallel pathways in thermodynamic terms.

In a previous study, the Glu24 → Ala mutation in the E24A variant of scMN was shown to have a subtle effect on both the energetics and structure of the TS on the slow pathway of folding and unfolding.<sup>50</sup> It seemed likely that E24A would display the signature upward curvature, either at very high denaturant concentrations or at low temperatures, where the degree of stabilization of the TS due to a weaker hydrophobic effect would be reduced. In this study, the unfolding of E24A has been characterized by both equilibrium and kinetic studies over a wide range of temperatures and denaturant concentrations. An upward curvature in the logarithm of its observed unfolding rate constant on denaturant concentration is seen at high guanidine hydrochloride (GdnHCl) concentrations, which is more pronounced at lower temperatures. This upward curvature has been interpreted to mean that, minimally, two pathways for unfolding are operative. Its observation has permitted a detailed thermodynamic analysis of the temperature and denaturant dependences of the unfolding kinetics, which has made it possible to determine how the TSs on the two pathways differ in their energies and compactness.

## MATERIALS AND METHODS

**Reagents and Protein Preparation.** All the reagents used were from Sigma and were of the highest purity grade. GdnHCl was purchased from USB and was of the highest purity grade. All the experiments were conducted in 50 mM phosphate buffer in the presence of 1 mM DTT and 0.25 mM EDTA (pH 7). The wild-type (wt) protein and the mutant variant (E24A) were purified as described previously.<sup>8,51</sup> The purity of the protein was confirmed by sodium dodecyl sulfate–polyacrylamide gel electrophoresis and mass spectrometry.

**Spectral Characterization Using Circular Dichroism (CD).** All the CD spectra were recorded using a Jasco J-815 spectropolarimeter. Far-UV spectra were acquired using a scan speed of 50 nm/min, a digital integration time of 2 s, and a bandwidth of 1 nm. Protein was used at a concentration of 10 μM in a cuvette with a 2 mm path length.

**Equilibrium Unfolding Studies.** GdnHCl-induced equilibrium unfolding studies were conducted by monitoring the change in the fluorescence of tryptophan using the MOS 450 optical system (Biologic) or by monitoring the change in the far-UV CD signal at 222 nm using the Jasco J-815 spectropolarimeter. Fluorescence emission was monitored at

340 nm using a 10 nm band-pass filter (Asahi Spectra), upon excitation at 280 nm. Protein was incubated at different temperatures in a water bath for up to 48 h, until it reached equilibrium. The temperature of the sample was controlled within ±0.5 °C, by using a circulating water bath for fluorescence measurements, and by using the attached Peltier system (PTC-423L) for far-UV CD measurements.

**Thermal Equilibrium Unfolding Studies.** Thermal equilibrium unfolding transitions were monitored using the change in the CD signal at 222 nm on the Jasco J-815 spectropolarimeter. The studies were conducted at 10 μM protein in a 2 mm cuvette, and the temperature scanning rate was 1 °C/min. The studies were conducted in the presence of 0.25–1.25 M GdnHCl.

**Unfolding Kinetics.** The unfolding of the E24A protein was studied using GdnHCl as a denaturant. The unfolding kinetic traces were monitored using the change in tryptophan fluorescence measured using the MOS optical system coupled to a stopped-flow module (SFM 4) from Biologic. The protein was excited at a wavelength of 280 nm, and emission was monitored at 340 nm using a 10 nm band-pass filter (Asahi Spectra). The dead time for mixing was 12 ms. The unfolding kinetics at low GdnHCl concentrations were studied using manual mixing with a dead time of 10 s. The final concentration of the protein was kept between 5 and 10 μM during unfolding. The temperature was controlled by circulating water through the stopped-flow module using a water bath. The fluctuation in temperature was <0.5 °C.

**Analysis of Equilibrium Unfolding Curves.** Discrete analysis of the equilibrium unfolding transitions of scMN was conducted using the two-state N ↔ U model, as described previously.<sup>8,45</sup> The value of the heat capacity change ( $\Delta C_p^U$ ) associated with the unfolding of the native protein was obtained by analyzing the plot of  $\Delta G_U$  versus temperature  $T$ , using the following equation.

$$\Delta G_U = \Delta H_m(1 - T/T_m) + \Delta C_p^U[T - T_m - T \ln(T/T_m)] \quad (1)$$

In eq 1,  $T_m$  is the melting temperature, at which the free energy of unfolding ( $\Delta G_U$ ) is zero.  $\Delta H_m$  is the value of the enthalpy change at  $T_m$ . All analysis was conducted using the CD-monitored equilibrium unfolding curves only.

**Analysis of Unfolding Kinetics.** Kinetic traces of unfolding were analyzed by fitting them to a single-exponential equation. The mechanism of unfolding of wt scMN can be represented by N ↔ I ↔ U, where the intermediate ensemble I forms rapidly in a millisecond burst phase reaction and is in a pre-equilibrium with N, defined by the equilibrium constant  $K_{NI}$ . The observed unfolding rate constant  $\lambda_U$  is given by

$$\lambda_U = \frac{K_{NI}}{K_{NI} + 1} k_U \quad (2)$$

In eq 2,  $k_U$  is the rate constant of unfolding of I. The value of  $K_{NI}$  changes exponentially with a change in GdnHCl concentration.<sup>52</sup> At lower GdnHCl concentrations, the pre-equilibrium favors N,<sup>50,52</sup> and  $K_{NI} \ll 1$ . However, at higher denaturant concentrations, the pre-equilibrium favors I,<sup>49</sup> and  $K_{NI} \gg 1$ . Under the latter condition, eq 2 reduces to the following equation.

$$\lambda_U = k_U \quad (3)$$

The dependence of  $k_U$  on denaturant concentration,  $[D]$ , was analyzed globally using the following equation that assumes the presence of two parallel pathways.<sup>5,39</sup>

$$k_U = k_U^{0,L} e^{m_{\ddagger-N}^L [D]} + k_U^{0,H} e^{m_{\ddagger-N}^H [D]} \quad (4)$$

In eq 4,  $k_U^0$  represents the observed rate constant for unfolding in the absence of denaturant and  $m_{\ddagger-N}$  represents the change in surface area between N and the TS of unfolding. It is assumed here that N and I do not differ significantly in their surface areas (see Discussion). The superscript letters L and H designate the two different pathways, which dominate at low and high GdnHCl concentrations, respectively.

**Global Analysis.** Global analysis of the equilibrium and kinetic data was conducted using a MATLAB program. The fitting parameters were allowed to vary and optimized using the function *fminsearchbnd* so as to achieve the lowest root-mean-square difference between all the experimental and simulated curves.

The denaturant-induced and thermally induced equilibrium unfolding transitions were globally fit to obtain the thermodynamic parameters. The thermodynamic parameters [ $\Delta H^\circ$ ,  $\Delta C_p^\circ$ , and  $T_m$  (at different denaturant concentrations)] and  $m_U$  were optimized to fit the experimental data. The analysis was conducted using a two-state equilibrium unfolding model<sup>8,45</sup> along with eq 1. The value of  $m_U$  was constrained to 2.9 kcal mol<sup>-1</sup> M<sup>-1</sup>, whereas all the other parameters were set free to vary.

To obtain the thermodynamic parameters for pathways L and H, the denaturant dependencies of the unfolding rate constant at different temperatures were globally fit to eqs 4 and 5:

$$\ln\left(\frac{k_U^0}{T}\right) = \ln(A) - \frac{1}{RT} \left\{ \Delta H_{T_0}^\ddagger - T \Delta S_{T_0}^\ddagger + \Delta C_p^\ddagger \left[ T - T_0 - T \ln\left(\frac{T}{T_0}\right) \right] \right\} \quad (5)$$

In eq 5,  $A$  is a pre-exponential factor, which represents the rate constant of unfolding in the absence of a barrier. While using eq 5 for analysis, the value of  $A$  was assumed to be 10<sup>6</sup> s<sup>-1</sup> and the value of  $T_0$  used was 298 K. The thermodynamic parameters ( $\Delta H^\ddagger$ ,  $\Delta S^\ddagger$ , and  $\Delta C_p^\ddagger$ ), the  $m_{\ddagger-N}$  values, and the dependencies of the  $m_{\ddagger-N}$  values on the temperature were optimized to fit the dependence of the observed rate constant. All the parameters were allowed to change within a range anticipated for a typical protein. All parameters were found to converge robustly, and none of the parameters hit the constraints of the global fit. It should be noted that the value of 10<sup>6</sup> s<sup>-1</sup> was chosen as the rate of unfolding in the absence of any energy barrier, as that was the value determined for folding reactions.<sup>53</sup> However, even when the value of  $A$  was varied between 10<sup>6</sup> and 10<sup>8</sup> s<sup>-1</sup>, the values of the thermodynamic parameters were found not to vary by more than 10%, and their dependencies on temperature were also found to be similar (data not shown).

## RESULTS

**Effect of Temperature on the Equilibrium Unfolding of E24A.** GdnHCl-induced equilibrium unfolding studies of E24A were conducted over a temperature range from 2 to 40 °C, using far-UV CD as the probe. Above 15 °C, the equilibrium unfolding transitions were also monitored using

fluorescence as the probe. In the temperature range in which both probes were used (15–40 °C), the fluorescence- and far-UV CD-monitored equilibrium unfolding transitions were found to overlap with each other. Figure 1 shows a

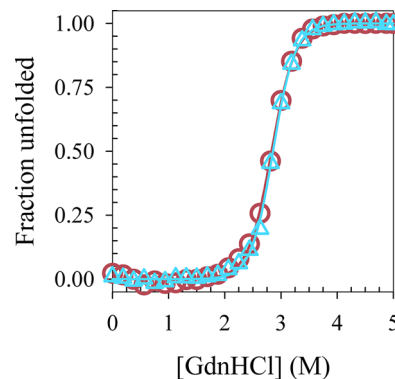


**Figure 1.** Equilibrium unfolding transitions of E24A monitored using different probes. Fluorescence-monitored (circles) and far-UV CD-monitored (triangles) equilibrium unfolding transitions at 25 °C obtained at 10 μM protein. The solid lines through the data represent fits to a two-state (N ↔ U) equilibrium unfolding model.<sup>45</sup>

representative comparison of the CD- and fluorescence-monitored equilibrium unfolding transitions at 25 °C. The fraction unfolded versus GdnHCl concentration plots obtained from far-UV CD-monitored equilibrium unfolding studies at different temperatures are shown in Figure 2a. Equilibrium unfolding transitions of E24A at all temperatures were analyzed using the two-state (N ↔ U) model. The  $m_U$  value does not change at temperatures above 20 °C but decreases with a decrease in temperature below 20 °C (data not shown). The decrease in the  $m_U$  value at lower temperatures influences the value of  $\Delta G_U^\circ$  and, hence, its dependence on temperature. To eliminate the variation caused by the change in the  $m_U$  value, global analysis was conducted by constraining the  $m_U$  value to the value obtained by averaging the  $m_U$  values obtained at temperature above 20 °C. Figure 2b shows thermally induced equilibrium unfolding transitions obtained in the presence of various concentrations of GdnHCl between 0.25 and 1.25 M. Thermal equilibrium unfolding studies in the absence of GdnHCl could not be conducted because of the irreversible precipitation of the protein at higher temperatures, but thermal transitions obtained in the presence of GdnHCl were fully reversible. Figure 2c shows the reversibility of thermal melting in the presence of 0.25 M GdnHCl. The midpoint ( $T_m$ ) of the thermal melt decreases with an increase in the concentration of GdnHCl.

GdnHCl-induced and thermally induced equilibrium unfolding transitions were globally fit to obtain thermodynamic parameters (Table 1). The protein appears to be most stable at ~9 °C (Figure 2d). For the analysis, the values of  $\Delta C_p^U$  and  $\Delta H^\circ$  were assumed to be independent of the GdnHCl concentration. The assumption seems valid, as the data were obtained over a small range of GdnHCl concentrations. For other proteins, it has been shown that  $\Delta C_p^U$  and  $\Delta H^\circ$  vary only very marginally with denaturant concentration.<sup>45,54–56</sup> Here it should be noted that even if the data obtained below 20 °C are ignored altogether in the global analysis, the values obtained for the thermodynamic parameters were found to be different by <10%, confirming the robustness of the global analysis.

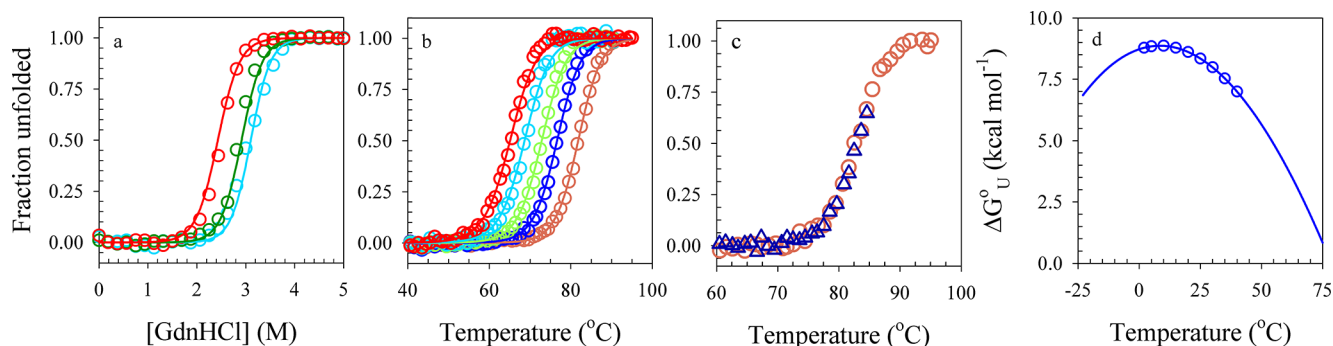


**Figure 2.** Thermodynamic characterization of the native state of E24A using CD spectroscopy. (a) Representative GdnHCl-induced equilibrium unfolding transitions obtained at 10 °C (blue circles), 25 °C (green circles), and 40 °C (red circles). (b) Thermal equilibrium unfolding transitions obtained at 0.25 M (dark red circles), 0.5 M (dark blue circles), 0.75 M (green circles), 1 M (light blue circles), and 1.25 M (light red circles). GdnHCl-induced and thermally induced equilibrium unfolding transitions were globally fit to obtain thermodynamic parameters for the unfolding of the native state. Solid lines through the data represent global fits to a two-state ( $N \leftrightarrow U$ ) equilibrium unfolding model.<sup>45</sup> (c) Reversibility of the thermal transition for unfolding in the presence of 0.25 M GdnHCl. A temperature-induced unfolding transition of the protein was acquired up to 85 °C (triangles). The unfolded protein was then allowed to refold upon rapid cooling. A second unfolding transition was then measured for the refolded protein (circles). The first (triangles) and second (circles) thermal transitions of the protein sample overlap with each other. (d) Temperature dependence of the free energy of unfolding ( $\Delta G^{\circ}_U$ ) derived from the thermodynamic parameters obtained from the global analysis of the data in panels a and b.

**Table 1. Kinetic and Thermodynamic Parameters Obtained from the Kinetic and Equilibrium Unfolding Studies of E24A at 25 °C<sup>a</sup>**

	kinetic unfolding studies		equilibrium studies
	pathway L	pathway H	
$m_{\ddagger-N}$	0.7 kcal mol <sup>-1</sup> M <sup>-1</sup>	1.7 kcal mol <sup>-1</sup> M <sup>-1</sup>	
$m_U$			3.0 kcal mol <sup>-1</sup> M <sup>-1</sup>
$\beta_T$ (from $m_U$ )	0.77	0.45	
$\Delta C_p^{\ddagger}$	0.25 kcal mol <sup>-1</sup> K <sup>-1</sup>	0.35 kcal mol <sup>-1</sup> K <sup>-1</sup>	
$\Delta C_p^U$			1.1 kcal mol <sup>-1</sup> K <sup>-1</sup>
$\beta_T$ (from $\Delta C_p^{\ddagger}$ )	0.78	0.69	
$\Delta S^{\ddagger}$	25 cal mol <sup>-1</sup> K <sup>-1</sup>	60 cal mol <sup>-1</sup> K <sup>-1</sup>	
$\Delta S^{\circ}$			64 cal mol <sup>-1</sup> K <sup>-1</sup>
$\Delta H^{\ddagger}$	26.5 kcal mol <sup>-1</sup>	43.3 kcal mol <sup>-1</sup>	
$\Delta H^{\circ}$			27 kcal mol <sup>-1</sup>

<sup>a</sup>Thermodynamic parameters for the activation of N to TS<sup>L</sup> (pathway L) and N to TS<sup>H</sup> (pathway H) were obtained by performing global analysis of the temperature dependencies of the unfolding rates along pathway L and pathway H, respectively, using eqs 4 and 5. The values of  $\beta_T$  were obtained from the values of  $m_{\ddagger-N}$  and  $m_U$ . The values of  $\Delta C_p^{\ddagger}$  for both the pathways were obtained from the global analysis. Thermodynamic parameters for the unfolding of N to U were obtained by performing global analysis of the thermally induced equilibrium unfolding transitions and GdnHCl-induced equilibrium unfolding transitions of E24A (Figure 2).

**Spectroscopic Properties of E24A Are Temperature-Independent.** The far-UV CD spectra of E24A overlap each other (Figure 3) across the range of temperatures being studied (2–40 °C), indicating that the native state does not undergo any gross structural change induced by the change in temperature.

**Dependence of Unfolding Rate Constants on GdnHCl Concentration.** Unfolding kinetic traces of wt scMN and E24A were acquired by monitoring the change in tryptophan fluorescence. The unfolding kinetics can be described as a

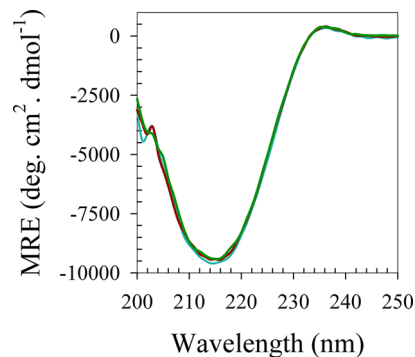


**Figure 3.** Comparison of the far-UV CD spectra of E24A at different temperatures and pH 7. Far-UV CD spectra of E24A obtained at 2 °C (blue), 20 °C (red), and 40 °C (green). Spectra were recorded at 10  $\mu$ M protein using a cuvette with a 2 mm path length.

three-state process. A burst phase fluorescence change takes place within 12 ms of mixing, followed by a single-exponential change in fluorescence. Figure 4a compares the kinetic and equilibrium amplitudes for the unfolding of E24A at 25 °C, whereas Figure 4b shows representative kinetic traces obtained at various GdnHCl concentrations at 25 °C. The unfolding rate constants obtained by fitting the unfolding kinetic traces to a single-exponential equation are shown in Figure 5. The plot of the logarithm of the unfolding rate constants versus GdnHCl concentration shows an upward curvature, and the curvature is more pronounced for E24A than for wt scMN (Figure 5a).

**Temperature Dependence of the Unfolding Kinetics of E24A.** Denaturant-induced kinetic unfolding studies were conducted at different temperatures. The unfolding kinetics gradually slows with a decrease in temperature from 45 to 10 °C. The upward curvature in the dependence of  $\log \lambda_U$  on GdnHCl concentration is evident at all temperatures and can be described by eq 4, which assumes two parallel pathways. The pathway that dominates at lower GdnHCl concentrations is designated as pathway L, while the pathway that dominates at higher GdnHCl concentrations is designated as pathway H. The  $m_{\ddagger-N}$  value for pathway L appears to be unchanged across the range of temperatures, while for pathway H, the  $m_{\ddagger-N}$  value

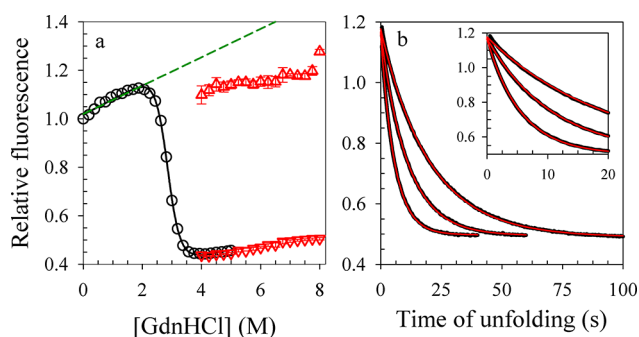


**Figure 4.** Comparison of the equilibrium and kinetic amplitudes of unfolding. (a) Equilibrium unfolding transition (O) and fit through the data (—) using a two-state  $N \leftrightarrow U$  model.<sup>45</sup> The upward-pointing triangles and downward-pointing triangles represent the  $t = 0$  and  $t = \infty$  values of relative fluorescence from the kinetic traces of unfolding, respectively, obtained by performing nonlinear least-square fits to the kinetic traces using a single-exponential equation. The green dashed line represents the extrapolated normalized signal for the native protein. The error bars represent the spreads of the measurements from at least two independent experiments. (b) Representative unfolding kinetic traces (—) obtained by unfolding the native protein at final GdnHCl concentrations of 7, 7.25, and 7.5 M (from right to left, respectively). The red lines through the curves represent nonlinear least-squares fits to a single-exponential equation. The inset shows the initial parts of the unfolding kinetic traces.

appears to decrease with an increase in temperature (Figure 5). GdnHCl concentration-dependent unfolding rate constants at all temperatures were globally fit to obtain the thermodynamic parameters governing the utilization of the parallel unfolding pathways (Table 1). The values obtained for the activation parameters governing unfolding to the TSs on the two pathways of E24A are similar in magnitude to the values obtained for unfolding to the TS on the single unfolding pathway observed for other proteins.<sup>41,43,57–60</sup>

## DISCUSSION

Because of the ensemble averaging nature of the probes used typically for protein folding and unfolding studies, the detection

of multiple pathways is not straightforward and often relies on indirect signatures in the observed kinetics.<sup>4,8,11–13,15,17,23,46,61,62</sup>  $\psi$ -value<sup>6</sup> and  $\phi$ -value analysis have also suggested the presence of parallel pathways, but in the latter case, the data were interpreted as anti-Hammond behavior,<sup>63</sup> even though the physical basis of the behavior was not explained.<sup>64</sup> Hydrogen exchange and cysteine labeling studies have also revealed parallel pathways.<sup>7,65–67</sup> Direct signatures for the presence of multiple pathways during protein folding<sup>9</sup> or protein unfolding<sup>5</sup> have been observed only rarely. Although parallel pathways for the folding and unfolding of monellin have been indirectly identified in previous studies,<sup>7,8,49</sup> it was not known what controlled the utilization of the different pathways. In this study, the E24A mutant variant of monellin, which was known to have an energetically perturbed TS for folding and unfolding,<sup>50</sup> was used to obtain the most direct signature of competing pathways. The observation of the upward curvature has allowed thermodynamic characterization of the TSs on the competing pathways, thereby leading to an understanding of how pathway switching can occur during folding or unfolding.

**Thermodynamic Properties of the Native State.** The detailed analysis of the thermally induced as well as GdnHCl-induced unfolding studies provides insights into the thermodynamic quantities that determine the free energy of unfolding. GdnHCl-induced equilibrium unfolding studies were conducted in the temperature range of 2–40 °C; at higher temperatures, both E24A and wt scMN precipitate out of solution. The fluorescence- and CD-monitored transitions are identical (Figure 1), indicating that equilibrium unfolding can be described as a two-state ( $N \leftrightarrow U$ ) process across the range of temperatures studied.

The observation that the  $m_U$  value of E24A is constant in the temperature range of 20–40 °C but decreases below 20 °C with a decrease in temperature (see Results) might suggest that the native structure is altered at lower temperatures, but this possibility is unlikely as the far-UV CD spectra of E24A do not change over the entire temperature range studied (Figure 3). Hence, the decrease in the  $m_U$  value must be either due to the presence of an equilibrium intermediate, which is significantly

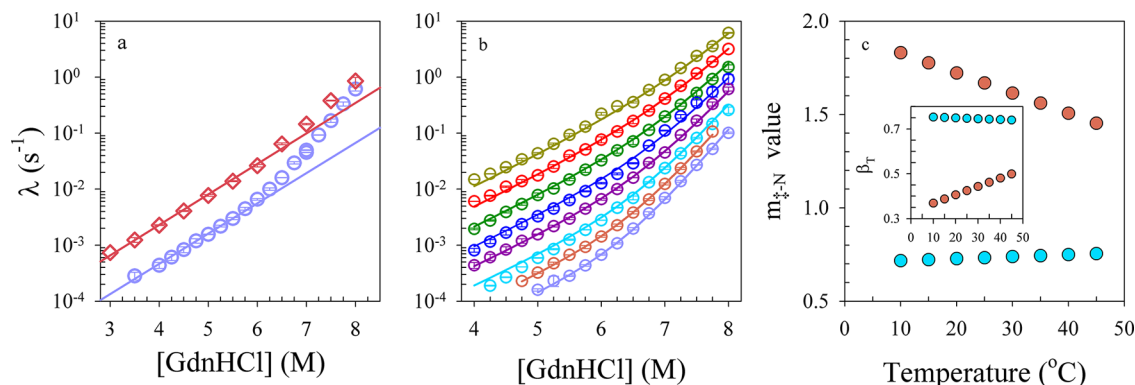


**Figure 5.** Dependence of the observed unfolding rate constants of monellin on GdnHCl at different temperatures. (a) Comparison of the observed unfolding rate constants obtained for wt scMN (diamonds) and E24A (circles) at 25 °C. The solid lines through the data are drawn by inspection only. (b) GdnHCl concentration dependencies of the observed rate constants determined at 10 °C (violet circles), 15 °C (dark red circles), 20 °C (light blue circles), 25 °C (maroon circles), 30 °C (dark blue circles), 35 °C (green circles), 40 °C (light red circles), and 45 °C (olive circles). The solid lines through the data represent global fits to the data, assuming two parallel pathways. The parameters obtained from fitting the data are listed in Table 1. (c) Temperature dependencies of the  $m_{\ddagger-N}$  values for pathway L (light blue circles) and pathway H (red circles), obtained from the global analysis of the kinetic unfolding data in panel b. The inset in panel c shows the temperature dependencies of the  $\beta_T$  values for pathway L (light blue circles) and pathway H (red circles). The error bars represent the spreads in measurement from at least two independent experiments.

populated only at lower temperatures, or due to an increase in the level of residual structure in the unfolded state with a decrease in temperature.

The temperature dependence of the free energy of unfolding of E24A determined in the absence of the GdnHCl shows that it is most stable at  $\sim 9$  °C. Global analysis of the GdnHCl-induced and thermally induced equilibrium unfolding transitions determined in the presence of different concentrations of GdnHCl yielded a value for  $\Delta C_p^U$  of  $1.1 \text{ kcal mol}^{-1} \text{ K}^{-1}$  (Table 1). It was found that even when the data obtained below  $20$  °C are ignored, the value obtained for  $\Delta C_p^U$  is found to be higher by  $<10\%$ , which indicates the robustness of the analysis. Indeed, the experimentally obtained value is in good agreement with the value for  $\Delta C_p^U$  of  $1.07 \text{ kcal mol}^{-1} \text{ K}^{-1}$  obtained from computational analysis<sup>68</sup> of the crystal structure of scMN. The value of  $T_m$  ( $352 \text{ K}$ ) in the absence of GdnHCl obtained from the analysis of the equilibrium unfolding transitions is close to the reported value of  $T_m$  ( $\sim 355 \text{ K}$ ) for wt scMN.<sup>69</sup>

**Unfolding Kinetic Mechanism of E24A.** The unfolding of wt scMN is known to begin with the formation of an intermediate (I) within the dead time of stopped-flow mixing.<sup>8,49,52</sup> This millisecond burst phase intermediate is significantly populated only at higher ( $>3 \text{ M}$ ) GdnHCl concentrations. It was shown to be a dry molten globule<sup>52</sup> based on observations from near-UV CD measurements that its tertiary structure is perturbed, from FRET measurements that it is slightly swollen compared to the native state, and from fluorescence experiments that it is dry in not possessing a hydrated hydrophobic surface capable of binding ANS.<sup>40</sup> Because I is a dry molten globule in being a marginally expanded form of the N state into which core water has not penetrated, its formation should not involve any significant change in surface area. Thus, the  $m$  value and the  $\Delta C_p$  value for the N to I transition should both be near zero.<sup>68</sup> Hence, the  $m_{\ddagger-N}$  and  $\Delta C_p^\ddagger$  values for the transition of I to the TSs are expected to be approximately the same as the values for the transition from N to the TSs. The fluorescence-monitored unfolding kinetics of E24A also shows a burst phase change in fluorescence followed by a single-exponential process, which in the case of E24A is slower than that seen for wt scMN. Although the burst phase intermediate populated during the unfolding of E24A has not been characterized, it is assumed to be the same I identified in the case of wt scMN.<sup>52</sup> There is no evidence of structural heterogeneity in I, as expected for a dry molten globule intermediate that differs from N mainly in possessing slightly loosened packing in the core. It is important to note the importance of the assumption that I is structurally homogeneous, because multiple pathways can arise due to structural heterogeneity in the population of the initial species, although only when the heterogeneous structures interconvert on a time scale that is slow compared to the unfolding time scale. This would be very unlikely in the case of a dry molten globule.

**Parallel Pathways for the Unfolding of E24A.** The observation that E24A displays a direct signature for the presence of parallel pathways in its unfolding kinetics, namely an unusual upward curvature in the dependence of the logarithm of the unfolding rate constant on GdnHCl concentration (Figure 5), is consistent with earlier observations that wt scMN utilizes multiple pathways to fold and unfold.<sup>8</sup> Such upward curvatures have been observed in previous unfolding<sup>5</sup> and refolding<sup>9</sup> studies. The unfolding kinetics have been analyzed with a minimal mechanism incorporating only

two competing pathways, which differ in their  $m_{\ddagger-N}$  values and in the stabilities of their TSs, and Figure 5 shows that this minimal mechanism is sufficient to describe the data and that there is no need to invoke additional pathways. The lower  $m_{\ddagger-N}^L$  value for pathway L compared to the  $m_{\ddagger-N}^H$  value for pathway H indicates that less surface area becomes solvent-exposed with the formation of  $\text{TS}^L$  than with the formation of  $\text{TS}^H$ . Thus,  $\text{TS}^L$  has a structure more compact than that of  $\text{TS}^H$ . In the case of I27, too, the TS on the unfolding pathway utilized at lower denaturant concentrations was found to be more compact than the TS on the unfolding pathway utilized at high denaturant concentrations.<sup>39</sup> The switch from pathway L with the more compact  $\text{TS}^L$  to pathway H with the less compact  $\text{TS}^H$ , with an increase in GdnHCl concentration, is responsible for the upward curvature in the case of monellin and I27.<sup>39</sup>

**Properties of the TSs along the Unfolding Pathways of E24A.** The observation that the value of  $\Delta C_p^\ddagger$  for the formation of  $\text{TS}^L$  is lower than that for the formation of  $\text{TS}^H$  from I (Table 1) is consistent with the interpretation from the  $m_{\ddagger-N}$  values that  $\text{TS}^L$  is more compact than  $\text{TS}^H$ . Unlike  $m$  values that are correlated with total surface area changes,  $\Delta C_p^\ddagger$  values are correlated more with nonpolar surface area changes.<sup>68</sup> Hence, more nonpolar surface area is exposed upon unfolding to  $\text{TS}^H$  than to  $\text{TS}^L$ . The values of  $\Delta C_p^\ddagger$  obtained for  $\text{TS}^L$  and  $\text{TS}^H$  are similar to the values reported for the transition states of other proteins.<sup>39,40,57,60</sup> The  $\beta_T$  value, which gives a measure of the compactness of the TS relative to the U (for which  $\beta_T = 0$ ) and N (for which  $\beta_T = 1$ ) states, can be calculated either from  $m$  values ( $\beta_T = 1 - m_{\ddagger-N}/m_U$ ) or from  $\Delta C_p^\ddagger$  values ( $\beta_T = 1 - \Delta C_p^\ddagger/\Delta C_p^U$ ). For pathway L, both measures yield the same value for  $\beta_T$  (Table 1), indicating that the same proportions of nonpolar and polar surface areas are exposed in  $\text{TS}^L$ , relative to those in the U. For pathway H, a higher  $\beta_T$  value is obtained from the  $\Delta C_p^\ddagger$  value than from the  $m_{\ddagger-N}$  value, indicating that proportionately less nonpolar surface area than polar surface area is exposed upon unfolding to  $\text{TS}^H$  than upon unfolding to U. In contrast, in a similar study with I27, the values of  $\beta_T$  obtained from  $m$  values and from  $\Delta C_p$  values were found to be in good agreement for both observed pathways.<sup>39</sup>

**The Glu24  $\rightarrow$  Ala Mutation Destabilizes the Dominant Unfolding Pathway.** In the native state, Glu24 is buried in the core of the protein, and it is responsible for the pH dependence of the stability of monellin.<sup>50</sup> The Glu24  $\rightarrow$  Ala mutation was found to stabilize the TS of unfolding at lower GdnHCl concentrations less than it stabilizes the native state.<sup>50</sup> This causes an increase in the height of the energy barrier for unfolding, leading to a decrease in the unfolding rate constant.<sup>50</sup> The  $m_{\ddagger-N}^L$  value for the unfolding pathway observed at lower denaturant concentrations in the case of E24A (pathway L) is the same as the  $m_{\ddagger-N}$  value observed for the wild-type protein,<sup>50</sup> suggesting that this pathway is the same for the two variants. Thus, the Glu24  $\rightarrow$  Ala mutation does not appear to alter the structure of the TS along the unfolding pathway, but it causes an increase in the height of the energy barrier for the unfolding of the protein. It appears that the mutation increases the activation free energy for pathway L, making it comparable to that for pathway H, which remains undetected for the wild-type protein, except perhaps at very high GdnHCl concentrations (Figure 5a). In the case of E24A, the TSs populated along the unfolding pathways are sufficiently different in their free energies to give rise to differences in the

unfolding kinetics but similar enough to allow their detection within the experimental denaturant concentration range. Furthermore, the TSs are sufficiently different in their compactness, which gives rise to different dependencies of the unfolding rate constants on denaturant concentration, to cause the upward curvature. The dependence of the observed unfolding rate constant of wt scMN on GdnHCl concentration also appears to have upward curvature (Figure 5a). This is less pronounced than that observed for E24A and appears only at GdnHCl concentrations above 7 M; hence, it was not observed in previous studies of unfolding at GdnHCl concentrations below 6 M.<sup>8,9</sup> The TS<sup>H</sup> found on pathway H of E24A is likely to be similar to the TS<sup>H</sup> apparent for wt scMN, but the latter can be observed in a range of GdnHCl concentrations that is too small to conduct any reliable characterization. It therefore appears that the Glu24 → Ala mutation does not significantly affect the stability of TS<sup>H</sup>. This is perhaps not surprising as the effect of the removal of the buried charge should be weaker on the stability of the less compact and more hydrated TS<sup>H</sup> than on the stability of the more compact and less hydrated TS<sup>L</sup>. In the case of I27, too, it was found that some mutations affected the kinetics of unfolding via only one of the two available pathways.<sup>39</sup>

**The Position of TS<sup>H</sup> Shifts along Pathway H with a Change in Temperature.** The simplest explanation for the decrease in the value of  $m_{\ddagger-N}^H$  for pathway H, and for the absence of any change in the value of  $m_{\ddagger-N}^L$  for pathway L, with an increase in temperature (Figure 5c) is that TS<sup>H</sup> becomes more compact at higher temperatures while the compactness of TS<sup>L</sup> does not change with a change in temperature. Because TS<sup>H</sup> is less compact with a hydrated hydrophobic surface (see above), and because hydrophobic interactions become stronger at higher temperatures,<sup>70,71</sup> it is expected to become more compact at higher temperatures. However, the observation that the stability of TS<sup>H</sup> decreases with an increase in temperature suggests that its compactness is not a dominant determinant of its stability. The observation that the value of  $m_U$  does not decrease with an increase in temperature makes it unlikely that the compactness of N changes with temperature. The structure of N also does not change with an increase in temperature (Figure 3), although it does become less stable. The observation that the value of  $m_{\ddagger-N}^H$  increases with an increase in temperature, while that of  $m_U$  remains unaltered, suggests that TS<sup>H</sup> shifts along the reaction coordinate to become more nativelike and compact at higher temperatures, in accordance with the Hammond postulate.<sup>72</sup> A temperature-dependent change in the kinetic  $m$  value was also observed in a previous study, where it was also interpreted as a shift in the position of TS.<sup>73</sup> At present, it is not known why the compactness of TS<sup>L</sup> does not change with a change in temperature, but this may be because TS<sup>L</sup> has relatively less nonpolar surface hydrated than does TS<sup>H</sup>, as indicated by the  $\Delta C_p^\ddagger$  values (Table 1).

**Entropies and Enthalpies of Activation.** More nonpolar surface area becomes solvated in TS<sup>H</sup> than in TS<sup>L</sup> (see the  $\Delta C_p^\ddagger$  values in Table 1); consequently, it is expected that there would be a greater loss of entropy as well as enthalpy during the formation of TS<sup>H</sup> than during the formation of TS<sup>L</sup>.<sup>74,75</sup> Nevertheless, the entropy of activation is positive for both pathway L and pathway H, and it is larger in magnitude for the latter (Table 1). Several other proteins also show a positive entropy of activation associated with the unfolding process.<sup>57–60</sup> The net increase in activation entropy suggests that the increase in entropy caused by the increased conformational

dynamics dominates over the decrease caused by solvation effects for unfolding to either TS. It is therefore not surprising that the net increase in entropy is greater in the less structured TS<sup>H</sup> than in the more structured TS<sup>L</sup>. Along pathway H, the large increase in entropy that takes place during unfolding to TS<sup>H</sup> is similar to the increase seen upon complete unfolding to U (Table 1). It appears that the increase in entropy consequent to an increase in conformational dynamics and the decrease in entropy due to hydration of nonpolar surface balance each other in such a manner that the net entropy gain is the same for the formation of TS<sup>H</sup> and U. In contrast, the entropy of unfolding to the less structured TS<sup>H</sup> in the case of I27<sup>39</sup> as well as that to the TS along the unfolding pathway of FKBP12<sup>41</sup> was found to be negative, indicating an entropic barrier and highlighting the important role of the solvent in the unfolding process.

For both pathway L and pathway H, the dominant contribution to the free energy of activation not only at 298 K but also over the entire accessible range of temperature is the enthalpic and not the entropic contribution (Figures 6b and 7).

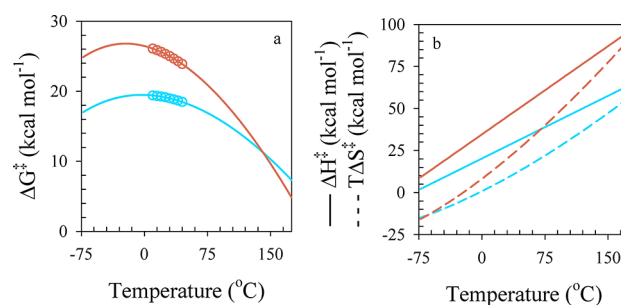


**Figure 6.** Thermodynamic properties of the two TSs along the parallel unfolding pathways of E24A. (a) Temperature dependence of the free energy of formation of the transition state ( $\Delta G^\ddagger$ ) in the absence of GdnHCl for pathway L (blue circles) and pathway H (red circles) obtained from the parameters listed in Table 1. (b) Temperature dependence of the  $\Delta H^\ddagger$  and  $T\Delta S^\ddagger$  values for the formation of TSs along pathways L (blue line) and H (red line).

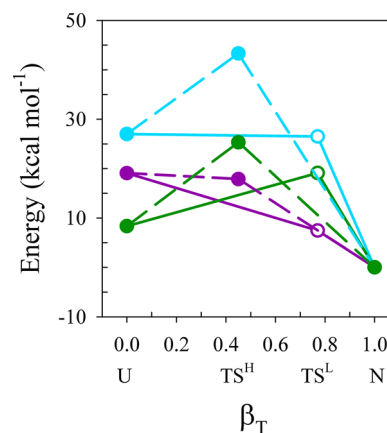


**Figure 7.** Thermodynamic characterization of the unfolding reactions along pathways L and H of the E24A variant of monellin. Contribution of the enthalpy [ $\Delta H^\circ$  (blue circles)] and the entropy [ $T\Delta S^\circ$  (maroon circles)] to the free energy [ $\Delta G^\circ$  (green circles)] profile of the unfolding reaction at 298 K in the absence of denaturant. Empty circles and solid lines represent data for pathway L, whereas filled circles and dashed lines represent data for pathway H. The  $\beta$  tanford ( $\beta_T$ ) value was calculated using the  $m$  values at 298 K.

The barriers on both pathways are therefore more enthalpic than entropic in origin. Both theoretical<sup>76,77</sup> and experimental<sup>40,59,78–80</sup> studies have, in fact, suggested the presence of enthalpic barriers in protein folding. Enthalpic barriers presumably arise when chain–solvent interactions have not yet compensated for intrachain interactions that have broken in the TSs. For unfolding to TS<sup>H</sup> at 298 K, the value for  $\Delta H^\ddagger$  is higher than the value of  $\Delta H^\circ$  for unfolding to U (Table 1 and Figure 7), which indicates the presence of an enthalpic barrier. For unfolding to TS<sup>L</sup>, the observation that the value of  $\Delta H^\ddagger$  at 298 K is comparable to the value of  $\Delta H^\circ$  for unfolding to U is probably just a consequence of the balance between the negative enthalpy of hydration of the nonpolar surface and the positive enthalpy associated with the breaking intrachain interactions being the same in TS<sup>L</sup> and U. The values of the enthalpies of activation along the two pathways for the unfolding of E24A are comparable in magnitude to the values reported for unfolding along the single pathways of other proteins.<sup>43,58,59</sup>

**Pathway L Is Identical to the Slow Pathway of Folding.** Previously, it was shown that for E24A, the effects of the Glu24 → Ala mutation on the free energies of activation for slow folding as well as unfolding predicted its effect on the free energy of unfolding.<sup>50</sup> Moreover, the amplitude of the slow folding pathway increased at the expense of those of the other folding pathways with an increase in GdnHCl concentration. These results made it possible to demonstrate that the pathway of unfolding at lower (<6 M) GdnHCl concentrations (pathway L) was identical to the slow pathway of folding.<sup>50</sup>

Neither the slow pathway of folding nor the fast and very fast pathways of folding of scMN display upward curvatures in the dependence of their observed folding rate constants on GdnHCl concentration,<sup>8</sup> as they do in the case of dcMN.<sup>9</sup> This may be either because folding rate constants were not determined at sufficiently low denaturant concentrations or because the population of a collapsed intermediate<sup>8</sup> obfuscates any upward curvature in the case of scMN. In the case of dcMN, upward curvatures were experimentally detectable, but only at very low GdnHCl concentrations, which were amenable for study because folding could be initiated by mixing of the two chains at low GdnHCl concentrations.<sup>9</sup> These observations highlight the point that this manifestation of multiple pathways requires that the TSs be different in both structure and energy in a very subtle manner.<sup>5,39</sup>

**Pathway Utilization Can Be Modulated.** In the absence of denaturant, TS<sup>L</sup> is significantly more stable than TS<sup>H</sup> (Figure 6a), and consequently, unfolding via pathway L is faster by more than 4 orders of magnitude than unfolding via pathway H, over the entire range of temperatures. Thus, although both pathways are available, the flux of unfolding molecules occurs so predominantly along pathway L that it is, in effect, the only pathway operational for E24A. It should be noted, however, that pathway H becomes the preferred pathway at high GdnHCl concentrations because the preferential free energy of interaction of GdnHCl is greater with TS<sup>H</sup> than with TS<sup>L</sup> (because  $m_{E-N}^H > m_{E-N}^L$ ). It is possible that in the cell, a chaperone, osmolyte or another chemical might also preferentially bind to the less structured TS<sup>H</sup> compared to the more structured TS<sup>L</sup>, thereby driving the reaction to follow pathway H. While this remains to be established in this case, it is important to point out that chaperones have been known to channel folding along one pathway when multiple pathways are available.<sup>81</sup>

## AUTHOR INFORMATION

### Corresponding Author

\*Phone: 91-80-23666150. Fax: 91-80-23636662. E-mail: jayant@ncbs.res.in.

### Funding

This work was funded by the Tata Institute of Fundamental Research and by the Department of Science and Technology, Government of India. J.B.U. is a recipient of a J. C. Bose National Fellowship from the Government of India.

### Notes

The authors declare no competing financial interest.

## ACKNOWLEDGMENTS

We thank members of our laboratory for discussion and Shachi Gosavi for her comments on the manuscript.

## ABBREVIATIONS

CD, circular dichroism; dcMN, double-chain monellin; scMN, single-chain monellin; GdnHCl, guanidine hydrochloride; TS, transition state.

## REFERENCES

- (1) Harrison, S. C., and Durbin, R. (1985) Is there a single pathway for the folding of a polypeptide chain? *Proc. Natl. Acad. Sci. U.S.A.* 82, 4028–4030.
- (2) Udgaonkar, J. B. (2008) Multiple routes and structural heterogeneity in protein folding. *Annu. Rev. Biophys.* 37, 489–510.
- (3) Bryngelson, J. D., Onuchic, J. N., Socci, N. D., and Wolynes, P. G. (1995) Funnels, pathways, and the energy landscape of protein folding: A synthesis. *Proteins* 21, 167–195.
- (4) Shastry, M. C., and Udgaonkar, J. B. (1995) The folding mechanism of barstar: Evidence for multiple pathways and multiple intermediates. *J. Mol. Biol.* 247, 1013–1027.
- (5) Wright, C. F., Lindorff-Larsen, K., Randles, L. G., and Clarke, J. (2003) Parallel protein-unfolding pathways revealed and mapped. *Nat. Struct. Biol.* 10, 658–662.
- (6) Krantz, B. A., Dothager, R. S., and Sosnick, T. R. (2004) Discerning the structure and energy of multiple transition states in protein folding using  $\psi$ -analysis. *J. Mol. Biol.* 337, 463–475.
- (7) Jha, S. K., Dasgupta, A., Malhotra, P., and Udgaonkar, J. B. (2011) Identification of multiple folding pathways of monellin using pulsed thiol labeling and mass spectrometry. *Biochemistry* 50, 3062–3074.
- (8) Patra, A. K., and Udgaonkar, J. B. (2007) Characterization of the folding and unfolding reactions of single-chain monellin: Evidence for multiple intermediates and competing pathways. *Biochemistry* 46, 11727–11743.
- (9) Aghera, N., and Udgaonkar, J. B. (2012) Kinetic studies of the folding of heterodimeric monellin: Evidence for switching between alternative parallel pathways. *J. Mol. Biol.* 420, 235–250.
- (10) Bhuyan, A. K., and Udgaonkar, J. B. (1998) Multiple kinetic intermediates accumulate during the unfolding of horse cytochrome c in the oxidized state. *Biochemistry* 37, 9147–9155.
- (11) Wildegger, G., and Kiefhaber, T. (1997) Three-state model for lysozyme folding: Triangular folding mechanism with an energetically trapped intermediate. *J. Mol. Biol.* 270, 294–304.
- (12) Mallam, A. L., and Jackson, S. E. (2007) A comparison of the folding of two knotted proteins: YbeA and YibK. *J. Mol. Biol.* 366, 650–665.
- (13) Radford, S. E., Dobson, C. M., and Evans, P. A. (1992) The folding of hen lysozyme involves partially structured intermediates and multiple pathways. *Nature* 358, 302–307.
- (14) Bilsel, O., Zitzewitz, J. A., Bowers, K. E., and Matthews, C. R. (1999) Folding mechanism of the  $\alpha$ -subunit of tryptophan synthase, an  $\alpha/\beta$  barrel protein: Global analysis highlights the interconversion of multiple native, intermediate, and unfolded forms through parallel channels. *Biochemistry* 38, 1018–1029.

- (15) Gianni, S., Travaglini-Allocatelli, C., Cutruzzola, F., Brunori, M., Shastry, M. C., and Roder, H. (2003) Parallel pathways in cytochrome  $c_{551}$  folding. *J. Mol. Biol.* 330, 1145–1152.
- (16) Roy, M., and Jennings, P. A. (2003) Real-time NMR kinetic studies provide global and residue-specific information on the non-cooperative unfolding of the  $\beta$ -trefoil protein, interleukin- $1\beta$ . *J. Mol. Biol.* 328, 693–703.
- (17) Kamagata, K., Sawano, Y., Tanokura, M., and Kuwajima, K. (2003) Multiple parallel-pathway folding of proline-free staphylococcal nuclease. *J. Mol. Biol.* 332, 1143–1153.
- (18) Stigler, J., Ziegler, F., Gieseke, A., Gebhardt, J. C., and Rief, M. (2011) The complex folding network of single calmodulin molecules. *Science* 334, 512–516.
- (19) Rami, B. R., and Udgaonkar, J. B. (2001) pH-jump-induced folding and unfolding studies of barstar: Evidence for multiple folding and unfolding pathways. *Biochemistry* 40, 15267–15279.
- (20) Sridevi, K., Lakshmikanth, G. S., Krishnamoorthy, G., and Udgaonkar, J. B. (2004) Increasing stability reduces conformational heterogeneity in a protein folding intermediate ensemble. *J. Mol. Biol.* 337, 699–711.
- (21) Brooks, C. L., III, Gruebele, M., Onuchic, J. N., and Wolynes, P. G. (1998) Chemical physics of protein folding. *Proc. Natl. Acad. Sci. U.S.A.* 95, 11037–11038.
- (22) Lakshmikanth, G. S., Sridevi, K., Krishnamoorthy, G., and Udgaonkar, J. B. (2001) Structure is lost incrementally during the unfolding of barstar. *Nat. Struct. Biol.* 8, 799–804.
- (23) Nguyen, H., Jager, M., Moretto, A., Gruebele, M., and Kelly, J. W. (2003) Tuning the free-energy landscape of a WW domain by temperature, mutation, and truncation. *Proc. Natl. Acad. Sci. U.S.A.* 100, 3948–3953.
- (24) Mello, C. C., and Barrick, D. (2004) An experimentally determined protein folding energy landscape. *Proc. Natl. Acad. Sci. U.S.A.* 101, 14102–14107.
- (25) Nishimura, C., Dyson, H. J., and Wright, P. E. (2002) The apomyoglobin folding pathway revisited: Structural heterogeneity in the kinetic burst phase intermediate. *J. Mol. Biol.* 322, 483–489.
- (26) Kloss, E., and Barrick, D. (2008) Thermodynamics, kinetics, and salt dependence of folding of YopM, a large leucine-rich repeat protein. *J. Mol. Biol.* 383, 1195–1209.
- (27) Zhou, B. R., Liang, Y., Du, F., Zhou, Z., and Chen, J. (2004) Mixed macromolecular crowding accelerates the oxidative refolding of reduced, denatured lysozyme: Implications for protein folding in intracellular environments. *J. Biol. Chem.* 279, 55109–55116.
- (28) Pradeep, L., and Udgaonkar, J. B. (2002) Differential salt-induced stabilization of structure in the initial folding intermediate ensemble of barstar. *J. Mol. Biol.* 324, 331–347.
- (29) Pradeep, L., and Udgaonkar, J. B. (2004) Effect of salt on the urea-unfolded form of barstar probed by m value measurements. *Biochemistry* 43, 11393–11402.
- (30) Sridevi, K., and Udgaonkar, J. B. (2002) Unfolding rates of barstar determined in native and low denaturant conditions indicate the presence of intermediates. *Biochemistry* 41, 1568–1578.
- (31) Wani, A. H., and Udgaonkar, J. B. (2009) Native state dynamics drive the unfolding of the SH3 domain of PI3 kinase at high denaturant concentration. *Proc. Natl. Acad. Sci. U.S.A.* 106, 20711–20716.
- (32) Du, F., Zhou, Z., Mo, Z. Y., Shi, J. Z., Chen, J., and Liang, Y. (2006) Mixed macromolecular crowding accelerates the refolding of rabbit muscle creatine kinase: Implications for protein folding in physiological environments. *J. Mol. Biol.* 364, 469–482.
- (33) Connell, K. B., Horner, G. A., and Marqusee, S. (2009) A single mutation at residue 25 populates the folding intermediate of *E. coli* RNase H and reveals a highly dynamic partially folded ensemble. *J. Mol. Biol.* 391, 461–470.
- (34) Magg, C., Kubelka, J., Holtermann, G., Haas, E., and Schmid, F. X. (2006) Specificity of the initial collapse in the folding of the cold shock protein. *J. Mol. Biol.* 360, 1067–1080.
- (35) Otzen, D. E., and Oliveberg, M. (1999) Salt-induced detour through compact regions of the protein folding landscape. *Proc. Natl. Acad. Sci. U.S.A.* 96, 11746–11751.
- (36) Capraro, D. T., Gosavi, S., Roy, M., Onuchic, J. N., and Jennings, P. A. (2012) Folding circular permutants of IL- $1\beta$ : Route selection driven by functional frustration. *PLoS One* 7, e38512.
- (37) Lindberg, M., Tangrot, J., and Oliveberg, M. (2002) Complete change of the protein folding transition state upon circular permutation. *Nat. Struct. Biol.* 9, 818–822.
- (38) Nauli, S., Kuhlman, B., and Baker, D. (2001) Computer-based redesign of a protein folding pathway. *Nat. Struct. Biol.* 8, 602–605.
- (39) Wright, C. F., Steward, A., and Clarke, J. (2004) Thermodynamic characterisation of two transition states along parallel protein folding pathways. *J. Mol. Biol.* 338, 445–451.
- (40) Agashe, V. R., Schmid, F. X., and Udgaonkar, J. B. (1997) Thermodynamics of the complex protein unfolding reaction of barstar. *Biochemistry* 36, 12288–12295.
- (41) Main, E. R., Fulton, K. F., and Jackson, S. E. (1999) Folding pathway of FKBP12 and characterisation of the transition state. *J. Mol. Biol.* 291, 429–444.
- (42) Zaman, M. H., Sosnick, T. R., and Berry, R. S. (2003) Temperature dependence of reactions with multiple pathways. *Phys. Chem. Chem. Phys.* 5, 2589–2594.
- (43) Segawa, S., and Sugihara, M. (1984) Characterization of the transition state of lysozyme unfolding. I. Effect of protein-solvent interactions on the transition state. *Biopolymers* 23, 2473–2488.
- (44) Chen, B. L., Baase, W. A., and Schellman, J. A. (1989) Low-temperature unfolding of a mutant of phage T4 lysozyme. 2. Kinetic investigations. *Biochemistry* 28, 691–699.
- (45) Agashe, V. R., and Udgaonkar, J. B. (1995) Thermodynamics of denaturation of barstar: Evidence for cold denaturation and evaluation of the interaction with guanidine hydrochloride. *Biochemistry* 34, 3286–3299.
- (46) Zaidi, F. N., Nath, U., and Udgaonkar, J. B. (1997) Multiple intermediates and transition states during protein unfolding. *Nat. Struct. Biol.* 4, 1016–1024.
- (47) Sanchez, I. E., and Kiefhaber, T. (2003) Evidence for sequential barriers and obligatory intermediates in apparent two-state protein folding. *J. Mol. Biol.* 325, 367–376.
- (48) Apetri, A. C., and Surewicz, W. K. (2002) Kinetic intermediate in the folding of human prion protein. *J. Biol. Chem.* 277, 44589–44592.
- (49) Jha, S. K., Dhar, D., Krishnamoorthy, G., and Udgaonkar, J. B. (2009) Continuous dissolution of structure during the unfolding of a small protein. *Proc. Natl. Acad. Sci. U.S.A.* 106, 11113–11118.
- (50) Aghera, N. K., Dasgupta, I., and Udgaonkar, J. B. (2012) A buried ionizable residue destabilizes the native state and the transition state in the folding of monellin. *Biochemistry* 51, 9058–9066.
- (51) Aghera, N., and Udgaonkar, J. B. (2011) Heterologous expression, purification and characterization of heterodimeric monellin. *Protein Expression Purif.* 76, 248–253.
- (52) Jha, S. K., and Udgaonkar, J. B. (2009) Direct evidence for a dry molten globule intermediate during the unfolding of a small protein. *Proc. Natl. Acad. Sci. U.S.A.* 106, 12289–12294.
- (53) Hagen, S. J., Hofrichter, J., Szabo, A., and Eaton, W. A. (1996) Diffusion-limited contact formation in unfolded cytochrome c: Estimating the maximum rate of protein folding. *Proc. Natl. Acad. Sci. U.S.A.* 93, 11615–11617.
- (54) Kumar, R., Prabhu, N. P., Yadaiah, M., and Bhuyan, A. K. (2004) Protein stiffening and entropic stabilization in the subdenaturing limit of guanidine hydrochloride. *Biophys. J.* 87, 2656–2662.
- (55) Felitsky, D. J., and Record, M. T., Jr. (2003) Thermal and urea-induced unfolding of the marginally stable lac repressor DNA-binding domain: A model system for analysis of solute effects on protein processes. *Biochemistry* 42, 2202–2217.
- (56) Nicholson, E. M., and Scholtz, J. M. (1996) Conformational stability of the *Escherichia coli* HPr protein: Test of the linear extrapolation method and a thermodynamic characterization of cold denaturation. *Biochemistry* 35, 11369–11378.

- (57) Jackson, S. E., and Fersht, A. R. (1991) Folding of chymotrypsin inhibitor 2. 2. Influence of proline isomerization on the folding kinetics and thermodynamic characterization of the transition state of folding. *Biochemistry* 30, 10436–10443.
- (58) Chen, X., and Matthews, C. R. (1994) Thermodynamic properties of the transition state for the rate-limiting step in the folding of the  $\alpha$  subunit of tryptophan synthase. *Biochemistry* 33, 6356–6362.
- (59) Kayatekin, C., Cohen, N. R., and Matthews, C. R. (2012) Enthalpic barriers dominate the folding and unfolding of the human Cu, Zn superoxide dismutase monomer. *J. Mol. Biol.* 424, 192–202.
- (60) Kuhlman, B., Luisi, D. L., Evans, P. A., and Raleigh, D. P. (1998) Global analysis of the effects of temperature and denaturant on the folding and unfolding kinetics of the N-terminal domain of the protein L9. *J. Mol. Biol.* 284, 1661–1670.
- (61) Bieri, O., Wildegger, G., Bachmann, A., Wagner, C., and Kiefhaber, T. (1999) A salt-induced kinetic intermediate is on a new parallel pathway of lysozyme folding. *Biochemistry* 38, 12460–12470.
- (62) de Prat-Gay, G., Nadra, A. D., Corrales-Izquierdo, F. J., Alonso, L. G., Ferreira, D. U., and Mok, Y. K. (2005) The folding mechanism of a dimeric  $\beta$ -barrel domain. *J. Mol. Biol.* 351, 672–682.
- (63) Matthews, J. M., and Fersht, A. R. (1995) Exploring the energy surface of protein folding by structure-reactivity relationships and engineered proteins: Observation of Hammond behavior for the gross structure of the transition state and anti-Hammond behavior for structural elements for unfolding/folding of barnase. *Biochemistry* 34, 6805–6814.
- (64) Daggett, V., Li, A. J., and Fersht, A. R. (1998) Combined molecular dynamics and  $\phi$ -value analysis of structure-reactivity relationships in the transition state and unfolding pathway of barnase: Structural basis of Hammond and anti-Hammond effects. *J. Am. Chem. Soc.* 120, 12740–12754.
- (65) Juneja, J., and Udgaonkar, J. B. (2002) Characterization of the unfolding of ribonuclease A by a pulsed hydrogen exchange study: Evidence for competing pathways for unfolding. *Biochemistry* 41, 2641–2654.
- (66) Ramachandran, S., Rami, B. R., and Udgaonkar, J. B. (2000) Measurements of cysteine reactivity during protein unfolding suggest the presence of competing pathways. *J. Mol. Biol.* 297, 733–745.
- (67) Arrington, C. B., and Robertson, A. D. (2000) Correlated motions in native proteins from MS analysis of NH exchange: Evidence for a manifold of unfolding reactions in ovomucoid third domain. *J. Mol. Biol.* 300, 221–232.
- (68) Myers, J. K., Pace, C. N., and Scholtz, J. M. (1995) Denaturant  $m$  values and heat capacity changes: Relation to changes in accessible surface areas of protein unfolding. *Protein Sci.* 4, 2138–2148.
- (69) Xue, W. F., Szczepankiewicz, O., Bauer, M. C., Thulin, E., and Linse, S. (2006) Intra- versus intermolecular interactions in monellin: Contribution of surface charges to protein assembly. *J. Mol. Biol.* 358, 1244–1255.
- (70) Privalov, P. L., and Gill, S. J. (1988) Stability of protein structure and hydrophobic interaction. *Adv. Protein Chem.* 39, 191–234.
- (71) Schellman, J. A. (1997) Temperature, stability, and the hydrophobic interaction. *Biophys. J.* 73, 2960–2964.
- (72) Hammond, G. S. (1955) A Correlation of Reaction Rates. *J. Am. Chem. Soc.* 77, 334–338.
- (73) Taskent, H., Cho, J. H., and Raleigh, D. P. (2008) Temperature-dependent Hammond behavior in a protein-folding reaction: Analysis of transition-state movement and ground-state effects. *J. Mol. Biol.* 378, 699–706.
- (74) Makhatadze, G. I., and Privalov, P. L. (1995) Energetics of protein structure. *Adv. Protein Chem.* 47, 307–425.
- (75) Privalov, P. L., and Makhatadze, G. I. (1993) Contribution of hydration to protein folding thermodynamics. II. The entropy and Gibbs energy of hydration. *J. Mol. Biol.* 232, 660–679.
- (76) Cheung, M. S., Garcia, A. E., and Onuchic, J. N. (2002) Protein folding mediated by solvation: Water expulsion and formation of the hydrophobic core occur after the structural collapse. *Proc. Natl. Acad. Sci. U.S.A.* 99, 685–690.
- (77) Rank, J. A., and Baker, D. (1997) A desolvation barrier to hydrophobic cluster formation may contribute to the rate-limiting step in protein folding. *Protein Sci.* 6, 347–354.
- (78) Chen, P., Long, J., and Searle, M. S. (2008) Sequential barriers and an obligatory metastable intermediate define the apparent two-state folding pathway of the ubiquitin-like PB1 domain of NBR1. *J. Mol. Biol.* 376, 1463–1477.
- (79) Liu, Z., and Chan, H. S. (2005) Desolvation is a likely origin of robust enthalpic barriers to protein folding. *J. Mol. Biol.* 349, 872–889.
- (80) MacCallum, J. L., Moghaddam, M. S., Chan, H. S., and Tieleman, D. P. (2007) Hydrophobic association of  $\alpha$ -helices, steric dewetting, and enthalpic barriers to protein folding. *Proc. Natl. Acad. Sci. U.S.A.* 104, 6206–6210.
- (81) Bhutani, N., and Udgaonkar, J. B. (2001) GroEL channels the folding of thioredoxin along one kinetic route. *J. Mol. Biol.* 314, 1167–1179.